

In summary, Yang and his group has demonstrated a novel approach to the synthesis of twisted lateral homostructures with orientation and phase conjunction turnabilities. This is a significant leap ahead of the conventional concept of epitaxy. With a patterned prototype device, they further demonstrated that the proposed approach is not only compatible with conventional lithography and etching processes, but also could be universally applied for fabricating various twisted complex materials. The results demonstrate the excellent controllability and unbounded conjunction tunability of the lateral homostructures using this method, which was subsequently named “weave epitaxy”. Such an approach not only provides a new way to design twisted lateral homostructures but also depicts an entirely different conceptual scene for epitaxial growth. (Reported by Yu-Chen Liu, National Cheng Kung University)

*This report features the work of Jan-Chi Yang and his collaborators published in Nat. Commun. 13, 2565 (2022).*

#### TPS 09A Temporally Coherent X-ray Diffraction

#### TPS 45A Submicron Soft X-ray Spectroscopy

#### TLS 13A1 X-ray Scattering

#### TLS 17A1 X-ray Powder Diffraction

#### TLS 17B1 X-ray Scattering

- XRD, XAS
- Materials Science, Condensed-matter Physics

#### Reference

1. P. C. Wu, C. C. Wei, Q. Zhong, S. Z. Ho, Y. D. Liou, Y. C. Liu, C. C. Chiu, W. Y. Tzeng, K. E. Chang, Y. W. Chang, J. Zheng, C. F. Chang, C. M. Tu, T. M. Chen, C. W. Luo, R. Huang, C. G. Duan, Y. C. Chen, C. Y. Kuo, J. C. Yang, Nat. Commun. **13**, 2565 (2022).

## CaCu<sub>3</sub>Ru<sub>4</sub>O<sub>12</sub>: An Unusually High-Kondo-Temperature Transition-Metal Oxide

*Using a combination of bulk sensitive hard and soft X-ray electron spectroscopy, the authors confirm that CaCu<sub>3</sub>Ru<sub>4</sub>O<sub>12</sub> is a high Kondo temperature metallic oxide.*

The Kondo effect involves the scattering of conduction-band electrons in a metal by localized magnetic impurities. It was originally observed as a minimum in electrical resistivity for a metal with magnetic impurities at low temperatures, along with coupled changes in the magnetic susceptibility and specific heat. Subsequently, the Kondo effect has been observed in many Ce, Yb, and U-based materials in which the localized magnetic 4f electrons hybridize with the conduction-band electrons and can lead to heavy fermion behavior.<sup>1</sup> However, the Kondo effect and heavy fermion behavior are rarely observed in oxides and LiV<sub>2</sub>O<sub>4</sub> is considered to be one such material.<sup>2</sup> More recently, the transition-metal oxide CaCu<sub>3</sub>Ru<sub>4</sub>O<sub>12</sub> (CCRO) has been considered as a Kondo material with heavy fermion behavior.<sup>3</sup> However, this hypothesis has been contested and debated in the literature.<sup>4</sup> In this highlight, through an international collaboration spanning Germany, Taiwan, Japan, Korea and Austria, researchers carried out a comprehensive study to determine whether

CCRO can be best described as a high-Kondo-temperature transition-metal oxide.<sup>5</sup>

The authors first carried out a careful comparison of the magnetic susceptibility of CCRO with that of CaCu<sub>3</sub>Ti<sub>4</sub>O<sub>12</sub> (CCTO). While the magnetic susceptibility of CCRO matched the data published in the literature, it exhibited an order of magnitude lower magnetic susceptibility compared with that of CCTO. This result implies that CCRO is nonmagnetic, in which case the Cu ions must be monovalent (with a non-magnetic 3d<sup>10</sup> configuration) or trivalent such as a nonmagnetic insulator NaCuO<sub>2</sub>. To confirm whether Cu ions in CCRO are magnetic, the authors carried out Cu L-edge X-ray absorption spectroscopy (XAS) and Cu 2p–3d resonant photoelectron spectroscopy (PES) at **TPS 45A1**, the Submicron Soft X-ray Spectroscopy beamline at the NSRRC, as shown in **Fig. 1** (see next page). The peak positions and line shape of the Cu L-edge XAS and the on-resonance 2p–3d PES spectra are typical of divalent Cu; hence, Cu in CCRO is not monovalent or trivalent.

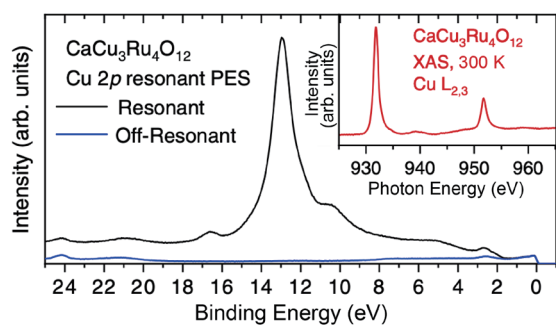


**Fig. 1:** Valence-band resonant photoelectron spectroscopy of  $\text{CaCu}_3\text{Ru}_4\text{O}_{12}$  with the experimental spectra recorded at the Cu 2p ( $L_3$ ) resonance ( $h\nu = 931.2$  eV) and at 10 eV below the resonance ( $h\nu = 921.2$  eV). The inset displays the experimental Cu- $L_{2,3}$  X-ray absorption spectrum. [Reproduced from Ref. 5]

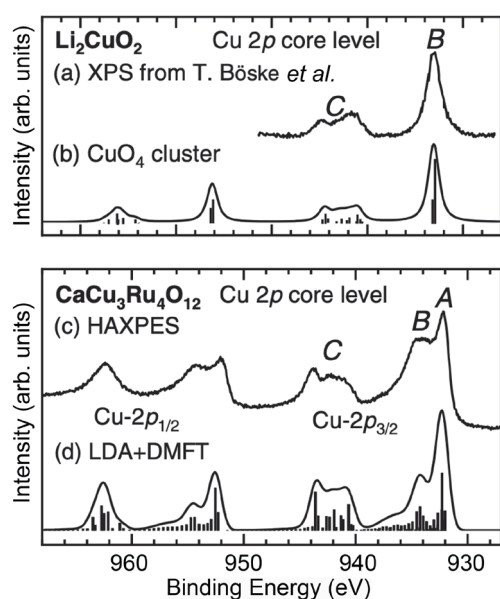


**Fig. 2:** Experimental Cu 2p core-level X-ray photoelectron spectrum of  $\text{Li}_2\text{CuO}_2$  reproduced from Ref. [1]. (b) Theoretical spectrum from the  $\text{CuO}_4$  cluster model. (c) Experimental Cu 2p core-level HAXPES spectrum of  $\text{CaCu}_3\text{Ru}_4\text{O}_{12}$ . (d) Theoretical spectrum from the LDA+DMFT method. [Reproduced from Ref. 5]

Next, the authors carried out Cu 2p core-level hard X-ray photoelectron spectroscopy (HAXPES) of CCRO and a reference material  $\text{Li}_2\text{CuO}_2$  at SP 12U1, the Taiwan-contract beamline at SPring-8, Japan, as shown in Fig. 2. CCRO and  $\text{Li}_2\text{CuO}_2$  comprise weakly coupled  $\text{CuO}_4$  plaquettes. It can be seen from Fig. 2 that, while the gross features are similar, there is a very important difference between the main peaks of CCRO and  $\text{Li}_2\text{CuO}_2$ : the CCRO main peak consists of two peaks, while  $\text{Li}_2\text{CuO}_2$  exhibits a single peak. The Cu 2p spectrum of  $\text{Li}_2\text{CuO}_2$  can be explained by a full multiplet calculation for a single  $\text{CuO}_4$ -cluster. On the other hand, the Cu 2p spectrum of CCRO cannot be explained in terms of a single  $\text{CuO}_4$ -cluster model. Furthermore, it also cannot be explained by a nonlocal screening mechanism, as it cannot accommodate inter-cluster hopping because the  $\text{CuO}_4$  plaquettes are isolated. The authors then showed that dynamical mean-field theory with local density

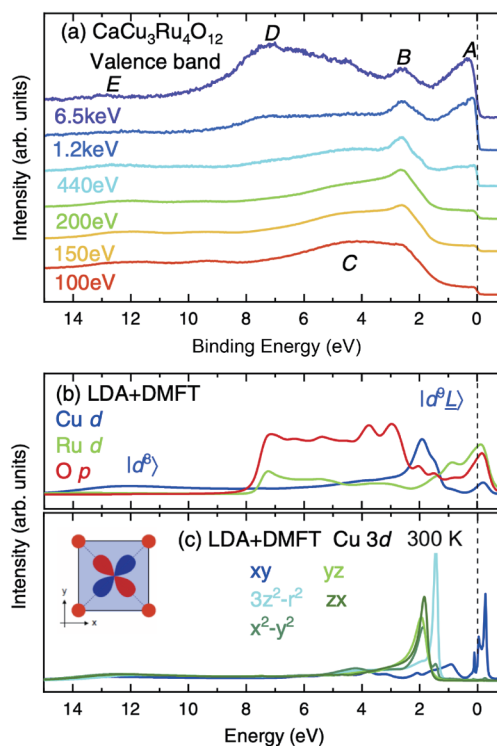


**Fig. 3:** Valence band spectra of  $\text{CaCu}_3\text{Ru}_4\text{O}_{12}$ : (a) experimental results measured at different photon energies and (b) LDA+DMFT spectral intensities for the Cu 3d, Ru 4d, and O 2p states. Spectral broadening is taken into account using a 200-meV Gaussian to simulate the experimental resolution. (c) LDA+DMFT spectral intensities of the Cu 3d orbitals in  $\text{CaCu}_3\text{Ru}_4\text{O}_{12}$ . The Cu orbitals are defined in the local axis of the  $\text{CuO}_4$  plane, as shown in the inset. [Reproduced from Ref. 5]

approximation (LDA+DMFT) calculations could explain the Cu 2p spectra. Thus, the authors inferred that CCRO contains correlated  $\text{Cu}^{2+}$  ions, which experience metallic screening.

Finally, the authors discuss the experimental valence-band spectra of CCRO measured using incident photon energies ranging from 100 eV to 6.5 KeV (Fig. 3(a)) and LDA+DMFT calculations that identify the partial density of states of Cu 3d, Ru 4d, and O 2p states in the valence-band spectra (Fig. 3(b)). As can be observed in Fig. 3(a), the valence band spectra reveal a systematic evolution with incident photon energy and, by taking into account photoionization cross-sections, features A and D are assigned to Ru 4d states, features B and E are assigned to Cu 3d states, and feature C can likely be assigned to the O 2p states. These assignments are confirmed by the LDA+DMFT results. Most interestingly, the authors also revealed that the Cu  $d_{xy}$  orbitals cross the Fermi level and are related to a small experimental feature just 0.07–0.08 eV above the Fermi level, which are obtained after dividing the experimental spectrum of CCRO by the metallic gold spectrum. This provides evidence for the Kondo-type behavior of CCRO and, from the optimized LDA+DMFT calculations, the authors could estimate a high Kondo temperature in the range of 500–1000 K.<sup>5</sup> The authors concluded by stating that “the material class

CaCu<sub>3</sub>M<sub>4</sub>O<sub>12</sub> indeed provides a unique opportunity to explore Kondo phenomena in transition metal compounds, where one may achieve lower Kondo temperatures by suitably varying the *M* constituent.” (Reported by Ashish Chainani)

*This report features the work of Liu Hao Tjeng, Atsushi Hariki and their collaborators published in Phys. Rev. X* **12**, 011017 (2022).

### TPS 45A1 Submicron Soft X-ray Spectroscopy SP 12U1 HAXPES/Photoemission

- Hard/Soft PES, XAS
- Condensed-matter Physics

#### References

1. G. R. Stewart, Rev. Mod. Phys. **56**, 755 (1984).
2. S. Kondo, D. C. Johnston, C. A. Swenson, F. Borsa, A. V. Mahajan, L. L. Miller, T. Gu, A. I. Goldman, M. B. Maple, D. A. Gajewski, E. J. Freeman, N. R. Dilley, R. P. Dickey, J. Merrin, K. Kojima, G. M. Luke, Y. J. Uemura, O. Chmaissem, J. D. Jorgensen, Phys. Rev. Lett. **78**, 3729 (1997).
3. W. Kobayashi, I. Terasaki, J.-i. Takeya, I. Tsukada, Y. Ando, J. Phys. Soc. Jpn. **73**, 2373 (2004).
4. H. Xiang, X. Liu, E. Zhao, J. Meng, Z. Wu, Phys. Rev. B **76**, 155103 (2007).
5. D. Takegami, C.-Y. Kuo, K. Kasebayashi, J.-G. Kim, C. F. Chang, C. E. Liu, C. N. Wu, D. Kasinathan, S. G. Altendorf, K. Hofer, F. Meneghin, A. Marino, Y. F. Liao, K. D. Tsuei, C. T. Chen, K.-T. Ko, A. Günther, S. G. Ebbinghaus, J. W. Seo, D. H. Lee, G. Ryu, A. C. Komarek, S. Sugano, Y. Shimakawa, A. Tanaka, T. Mizokawa, J. Kuneš, L. H. Tjeng, A. Hariki, Phys. Rev. X **12**, 011017 (2022).

## High-Speed and Energy-Efficient Electronics

*The coexistence of a topological surface state and a Rashba surface state in a Dirac semimetal,  $\alpha$ -Sn, may significantly enhance the potential for spintronic applications.*

The diverse topological phases of matter have been studied in detail, not only out of scientific interest, but also for their potential applications. Indicated by their special Dirac cones in the band structure, novel quantum oscillations are frequently observed in systems hosting Dirac fermions. Applications utilizing these Dirac states are now being extensively investigated in many fields, including thermoelectric devices, photonic devices, spin-based field-effect transistors, and memories, etc. A group IV element with a diamond structure,  $\alpha$ -Sn is one of the materials that provides an ideal platform for realizing abundant topological phases based on its non-trivial band topology. Moreover, a large spin-to-charge conversion at room temperature has been demonstrated *via* spin pumping, while an efficient current-induced magnetization switching was achieved in  $\alpha$ -Sn/magnetic metal heterostructures, thus making  $\alpha$ -Sn attractive for spintronic applications.

In the exploration of topological phase transitions, bandgap engineering *via* quantum confinement effects or strain modulation has been a commonly used approach in addition to chemical doping. Band evolution in a few layers of thin films attracts great attention since the confinement effect has a significant influence on the bandgap. A thickness-dependent topological phase transition often occurs when the system undergoes a band inversion during the bandgap engineering. A single-layer  $\alpha$ -Sn, especially in the (111) orientation, is of great interest because of its honeycomb-like structure in analogy to graphene and its large quantum-spin-Hall gap. As the film becomes thicker, a two-dimensional to three-dimensional (3D) band transition takes place and the unstrained  $\alpha$ -Sn becomes a zero-gap semiconductor. Besides the interesting phase transition found in  $\alpha$ -Sn(111), the band evolution in the (001) orientation is also worth studying but has yet to be fully explored in a wide thickness range.

To deepen understanding of the evolution of topological transition in  $\alpha$ -Sn(001) for increasing thickness, Raynien Kwo (National Tsing Hua University), Cheng-Maw Cheng (NSRRC) and their teams studied the electronic structure of in-plane compressively strained  $\alpha$ -Sn(001) on InSb(001) substrates with varying thicknesses ranging from a few bilayers (BL) to 370 BLs. Comprehensive angle-resolved photoemission spectroscopy (ARPES) experiments at **TLS 21B1** were carried out on high-quality  $\alpha$ -Sn thin films prepared using molecular beam epitaxy (MBE). A critical thickness of 5–6 BLs for the transition between topologically trivial and non-trivial phases was experimentally determined for the first time in undoped  $\alpha$ -Sn(001) thin films. As the film thickness exceeded 30 BLs, additional Rashba-like surface states (RSS) were newly identified and could be associated with the preformed topological surface states (TSS) in the phase transition to a 3D topological insulator (TI). Moreover, they compared with the density functional theory (DFT) calculations and found the 3D Dirac nodes at  $k_z \approx 0.0276$